International Journal of Mass Spectrometry 438 (2019) 63–71

Contents lists available at ScienceDirect

International Journal of Mass Spectrometry

journal homepage: www.elsevier.com/locate/ijms

Full Length Article

Dissociative photoionization of chromium hexacarbonyl: A round-trip ticket to non-statisticality and a detective story in thermochemistry☆

Krisztina Voronova[a,1], Krisztián G. Torma[a], James P. Kercher[b], Andras Bodi[c], Bálint Sztáray[a,*]

[a] Department of Chemistry, University of the Pacific, Stockton, CA 95211, USA
[b] Department of Chemistry, Hiram College, Hiram, OH 44234, USA
[c] Laboratory for Synchrotron Radiation and Femtochemistry, Paul Scherrer Institute, 5232 Villigen, Switzerland

ARTICLE INFO

Article history:
Received 15 August 2018
Received in revised form
27 November 2018
Accepted 14 December 2018
Available online 17 December 2018

Keywords:
Photoionization
Unimolecular dissociation
Non-statisticality
Thermochemistry
PEPICO

ABSTRACT

The fragmentation processes of internal energy selected chromium hexacarbonyl cations, $Cr(CO)_6^+$, were investigated by imaging photoelectron photoion coincidence (iPEPICO) spectroscopy at the VUV beamline of the Swiss Light Source. In the 9.3–21.5 eV photon energy range, $Cr(CO)_6^+$ dissociates by six sequential carbonyl ligand losses. The fragment ion fractional abundances, plotted in the breakdown diagram, along with the time-of-flight mass spectra for the first three metastable CO-loss channels were modeled using a statistical approach. Between 12 and 16 eV, the statistical model overestimates the degree of fragmentation, which is explained by enhanced kinetic energy release in impulsive CO loss on repulsive electronic states of the parent ion $Cr(CO)_6^+$, as confirmed by TD-DFT calculations. This is the first reported example for an embedded non-statistical unimolecular dissociation regime, bracketed by statistical regimes at low and at high energies. The statistical model was employed to derive 0 K appearance energies for $Cr(CO)_n^+$ (n = 0–5). The $Cr(CO)_5^+$ appearance energy and the literature CO—$Cr(CO)_5^+$ bond dissociation energy yield an adiabatic $Cr(CO)_6^+$ ionization energy of 8.195 ± 0.120 eV, independent of photoelectron spectroscopy measurements. The 0 K appearance energy of Cr^+ is 61 kJ mol^{-1} higher than predicted based on literature enthalpies of formation, which we suggest is most likely due to an error in the enthalpy of formation of $Cr(CO)_6$, and propose a revised $\Delta_f H[Cr(CO)_6, g] = -972.1 \pm 4.1$ and -968.9 ± 4.1 kJ mol^{-1} at 0 and 298 K, respectively, and $\Delta_f H_{298K}[Cr(CO)_6, c] = -1040.6 \pm 4.2$ kJ mol^{-1} for the crystalline state, based on the known enthalpy of sublimation. The measured Cr—CO bond dissociation energies in $[(CO)_nCr—CO]^+$ (n = 0–5), and the enthalpies of formation of the chromium carbonyl ion series are also reported.

1. Introduction

Chromium hexacarbonyl, $Cr(CO)_6$, is an ideal model system for understanding coordination, bonding, and reactivity in organometallic compounds [1–3]. It is the starting material for the synthesis of $Cr(arene)(CO)_3$ complexes, which are among the most studied organometallic compounds because of their application in aromatic synthesis [4].

Several theoretical [5–11] and experimental [12–21] studies have been carried out to explore the structure and obtain sequential bond dissociation energies, BDE, for $Cr(CO)_6$ and its $Cr(CO)_n^+$ (n = 0–6) ions. However, the reported BDE and appearance energies, E_0, vary widely, by up to 1.8 eV, from one study to another. This was pointed out by Armentrout et al. [12], in a paper that also reported the Cr—CO bond energies, measured in individually mass-selected $Cr(CO)_n^+$ ions by threshold collision-induced dissociation (TCID) in a guided ion beam tandem mass spectrometer. The sum of the six ionic bond dissociation energies, 4.99 ± 0.14 eV, was compared to the literature reaction enthalpy for dissociating all six ligands from the $Cr(CO)_6^+$ cation, 5.05 ± 0.09 eV at 0 K. The latter value is based on the precursor complex's heat of formation from calorimetry and its ionization energy, IE, from photoelectron spectroscopy experiments [22]. This very good agreement appears to be all the more reassuring in the light of the unusually small, 1.7 kJ mol^{-1} (0.017 eV), uncertainty in the chromium hexacarbonyl enthalpy of formation as reported in the literature [22]. In contrast, previous photoionization studies, *e.g.*, by Meisels et al. [16] and Michels et al. [17], obtained up to ≈1.8 eV higher sum of BDE,

☆ Helmut Schwarz Honour Issue.
* Corresponding author.
E-mail address: bsztaray@pacific.edu (B. Sztáray).
[1] Current address: Department of Chemistry, University of Nevada, Reno, NV 89557-0216, USA.

https://doi.org/10.1016/j.ijms.2018.12.010
1387-3806/

in seemingly glaring disagreement with the calorimetry literature. Although we will argue that the 0.09 eV uncertainty of the literature-based 5.05 eV dissociation energy is a result of selective averaging of a small subset of the numerous experimental results, the previous photoionization results [14,13–21] still seem to be in error. This is likely due to disregarding the excess energy partitioning between each sequential CO-loss fragment ions and the leaving CO neutral molecules, which leads to a higher reported appearance energy for the Cr^+ ion. This point is underlined by our finding that, while the excess energy partitioning is statistical in most of the photon energy range, it is clearly non-statistical due to impulsive dissociation around 14 eV of photon energy, a phenomenon not reported before.

Photoionization studies of $Cr(CO)_6$ were also carried out by Qi et al. [14] and Ng et al. [15] using synchrotron radiation and time-of-flight mass spectrometry. The photoionization efficiency (PIE) curves for the $Cr(CO)_n^+$ ions were measured, from which the ionization energy and the appearance energies were determined. These studies reported bond dissociation energies that were in reasonable agreement with the earlier photoionization data. However, the sums were again much too high by up to ≈1.4 eV when compared to the calorimetry results, see Table 2.

Muntean and Armentrout [13] reinvestigated the TCID of $Cr(CO)_6^+$ and provided a slightly revised BDE value for the first CO-loss. This change put their sum of bond dissociation energies to 5.07 ± 0.15 eV (for which we have recalculated the confidence interval, based on the reported uncertainties of the underlying data). This report further improved the agreement with the cited 5.05 ± 0.09 eV literature enthalpy difference between the chromium ion plus six CO molecules and chromium hexacarbonyl.

Both photoelectron photoion coincidence spectroscopy (PEPICO) and TCID are well-established techniques to obtain reliable thermochemistry by complimentary approaches. In the recent study of the dissociative photoionization of iron pentacarbonyl, $Fe(CO)_5$ [23], it was demonstrated that PEPICO and TCID experiments were consistent if the kinetic shifts, the initial parent ion internal energy distribution, and the excess energy distribution are all taken into account in the data analysis of the former. As far as organometallic compounds are concerned, PEPICO was used, for example, to establish trends in manganese chalcocarbonyl bond energies [24] and the effect of phosphine analogue ligands on metal–carbonyl bond energies in cobalt complexes [25]. Both approaches can be used to study binary carbonyls of, *e.g.,* iron [23], chromium [12,13], and platinum [26]. TCID can also be used to study reactivities of a metal center, *e.g.,* alkane activation by gas phase molybdenum ions [27]. Since both approaches yield energetics data directly, they can also be combined to construct thermochemical cycles to unveil the thermochemistry of organometallic complexes impervious to both calculations and conventional thermochemical measurements [28].

In threshold PEPICO, internal energy selected photoions are produced in the gas phase by threshold ionization using tunable vacuum ultraviolet (VUV) radiation and their dissociation is analyzed by time-of-flight (TOF) mass spectrometry [29]. A breakdown diagram is constructed by plotting the fractional ion abundances as a function of the ionizing photon energy, which corresponds to varying the internal energy of the parent ion. The 0 K appearance energies can then be determined by statistical modeling of the breakdown diagram as well as the dissociation rate constants when kinetic shifts must be accounted for. In the case of slow unimolecular reactions compared to the time scale of the ion mass analysis, asymmetric fragment ion peak shapes carry the unimolecular dissociation rate information, to which the statistical model is fitted in the data analysis. In addition, the energy taken away by the leaving neutral fragments has to be taken into account and the resulting broadening of the breakdown curves can be accurately modeled, as demonstrated by numerous recent PEPICO studies [23,30]. *Nota bene*, this broadening effect is also clearly observable in the breakdown diagram of Meisels et al. [16].

In this study, we have revisited the dissociative photoionization of energy selected $Cr(CO)_6^+$ cations using imaging PEPICO (iPEPICO) spectroscopy, as implemented using synchrotron radiation at the VUV beamline of the Swiss Light Source, to determine accurate appearance energies and ionic metal-carbonyl bond dissociation energies.

2. Experimental section

$Cr(CO)_6$ was purchased from Sigma–Aldrich and measured using the iPEPICO spectrometer [31] at the VUV beamline [32] of the Swiss Light Source. $Cr(CO)_6$ was introduced directly in the ionization chamber at room temperature through a Teflon tube from the headspace of a glass vial. Synchrotron VUV light was collimated, dispersed in grazing incidence by a 600 or 1200 grooves/mm laminar grating, depending on the photon energy, and focused at a 200 μm exit slit in a differentially pumped gas filter with a photon energy resolution of 3–5 meV. Higher-order harmonic radiation was suppressed by a 10 cm long chamber in the gas filter filled with 10 mbar of a Ne–Ar mixture or Ne, depending on the wavelength. The photon energy was calibrated using 11s′–14s′ Ar and 13s′–13d′ Ne autoionization lines in first and second order of the diffraction grating. The effusive sample beam was intersected with the monochromatic VUV synchrotron radiation in the experimental chamber, ionizing the sample in a 2 mm × 2 mm cross-section interaction region at a typical pressure of $2–4 \times 10^{-6}$ mbar. A constant 40 V cm^{-1} electric field was used to extract photoions and photoelectrons in opposite directions. Electrons were kinetic energy analyzed using velocity map imaging and a Roentdek DLD40 position sensitive delay-line detector with sub-meV kinetic energy resolution at threshold and provided the start signal for the ion time-of-flight analysis. Photoions were detected by a Jordan TOF C-726 microchannel plate detector after a two-stage Wiley–McLaren time-of-flight mass analyzer [33] with 5.5 cm long extraction, 1 cm long acceleration, and 55 cm drift regions. The long extraction region and the low extraction field result in ion residence times on the order of several μs and metastable parent ions yield quasi-exponential TOF peak shapes, characteristic of the first-order dissociation rate constants [34]. Electron hit times and positions, and ion hit times were correlated using a multiple-start/multiple-stop data acquisition scheme [35]. “Hot,” that is, non-threshold, kinetic energy photoelectrons with a small off-axis momentum component are selected in a ring area around the threshold, center spot in an approximately three times larger surface area. Threshold electrons and hot electrons with no off-axis momentum component are both detected in the image center and the contribution of the latter was approximated by the average count rate in the ring area around the center spot. In the data analysis, the coincidence spectrum corresponding to the ring electron detector was subtracted from the center signal, to obtain threshold photoionization mass spectra [36] and to construct the breakdown diagram based on fractional ion abundances as a function of photon energy.

The Gaussian 09 suite of programs was used to carry out quantum chemical calculations on $Cr(CO)_6$, its molecular ion, and fragment ions [37]. The geometries of neutral and ionic species were optimized using density functional theory with the B3LYP functional and the 6-311++G(d,p) basis set, which provided input parameters for the statistical model. In addition, reaction energy curves along the optimized CO-loss coordinate were calculated at the M06-2X/def2-TZVPP and B3LYP/6-311++G(d,p) levels of theory. Finally, two EOM-EE-CCSD/cc-pVDZ calculations were carried out at the equilibrium and elongated Cr—C bond lengths using the Q-Chem 4.3 program package to check the nature of different spin

states with respect to CO-loss [38]. Vibrational frequencies and rotational constants were used to calculate the a) thermal energy distribution of the neutral precursor molecules; b) densities and numbers of states for the statistical rate equation; c) to obtain the statistical product energy distributions upon the sequential dissociations [39]. The calculated harmonic vibrational frequencies were used as input for the PEPICO data analysis in the statistical model [34].

We used the simplified statistical adiabatic channel model (SSACM) to calculate metastable dissociation rates in modeling the breakdown diagrams and ion time-of-flight distributions [34]. The unimolecular rate constants, $k(E)$, can be calculated as

$$k(E) = \frac{\sigma N^{\ddagger}(E - E_o)}{h\rho(E)},$$

where σ is the reaction symmetry, $N^{\ddagger}(E - E_0)$ is the sum of states of the transition state from 0 to $E - E_0$, h is Planck's constant, and $\rho(E)$ is the density of states of the parent ion at energy E [39]. The densities and sums of states are calculated using harmonic vibrational frequencies by the Beyer–Swinehart direct count algorithm [40]. It was shown earlier that the extrapolation to the dissociation onset is more reliable using the SSACM model if the kinetic shift is larger than 200 meV, in particular when the reaction energy curve is attractive, *i.e.* without a maximum corresponding to the transition state [41]. In SSACM, the product vibrational frequencies and moments of inertia are used to calculate $N^{\ddagger}(E - E_0)$. The rigidity factor, $f_{\text{rigid}}(E)$, is then employed to prevent the rate constant from rising too rapidly with increasing ion internal energy. The rigidity factor takes the following form:

$$f_{\text{rigid}}(E) = \left(1 + \left(\frac{(E - E_o)}{c}\right)^2\right)^{-\frac{2}{3}},$$

where c is the fitting parameter adjusted to fit the experimental data together with the dissociation onset [34].

After each CO loss, the excess energy above the dissociation barrier is assumed to be distributed statistically according to the relative phase space volumes between the fragment ion, the leaving CO and the newly formed translational degrees of freedom. This broadens the internal energy distribution and leads to the slight broadening of the breakdown curves with increasing fragmentation [39].

3. Results and discussion

3.1. Modeling the consecutive dissociation processes

Time-of-flight mass spectra of internal energy selected chromium hexacarbonyl cations were collected in the 9.3–21.5 eV photon energy range, in which $Cr(CO)_6^+$ dissociates *via* six sequential CO-loss reactions.

The adiabatic ionization energy of $Cr(CO)_6$ is ancillary input in the statistical model, which defines the origin of the parent ion density of states in the rate equation and it would be directly needed to derive the first Cr—CO^+ bond dissociation energy, based on the optimized first appearance energy. It has been measured by electron ionization [17,18,20,42] and photoionization [14,16,43,44] experiments to be between 8.10–8.48 eV. The hot band corrected value of 8.142 ± 0.017 eV by Lloy and Schlang [43] from 1969 was recommended by Lias et al. [45] in their compilation in 1988. However, the identification of the 0–0 origin band is not definitive [46]. An IE of 8.24 ± 0.07 eV was obtained in a PEPICO experiment by Meisels and co-workers [16], in agreement with an inflection point at 8.24 eV noted by Lloy and Schlang [43]. First in 1993 and later in 2001, Armentrout et al. [12,13] used 8.19 ± 0.07 eV, the average of the photoionization values by Meisels et al. [16] and Lloy and Schlang [43], to calculate the heat of formation of the $Cr(CO)_6^+$ ion. The latest experimentally determined IEs were reported as 8.157 ± 0.026 eV and 8.10 ± 0.01 eV by Ng et al. [15] and Qi et al. [14], respectively, both obtained by linear extrapolation of the photoionization efficiency curves. The former is in reasonably good agreement with the value recommended by Armentrout et al. [12,13], while the latter is the lowest one in the literature, matching the Hubbard and Lichtenberger determination [44] from 1982.

It is not surprising, however, that there is considerable disagreement over the IE in the literature. The first ionization band of organometallics is typically a broad and featureless peak, corresponding to ionization from a *d* orbital yielding three doublet states, each affected by spin-orbit coupling. Therefore, the *d*-band usually lacks sufficient fine structure to employ Franck–Condon simulations to determine an accurate adiabatic ionization energy. So as not to mix the rather qualitative analysis of the photoelectron spectrum with the quantitative analysis of dissociative photoionization, we have not recorded the TPES. In this work, for consistency, we first checked the IE value from Armentrout et al. [12,13] and then, rather than using this uncertain IE from photoelectron spectroscopy, determined the first CO-loss appearance energy, E_0, by fixing the first ionic BDE to the TCID value and optimized the IE to fit the breakdown curve for $Cr(CO)_5^+$. In the rest of the statistical model, this IE value was then used to calculate the internal energy distribution of the molecular ion. It is important to note here that the choice of IE only affects the first BDE directly and its effects on the rest of the BDEs are close to negligible.

The breakdown diagram is shown in Fig. 1 and selected threshold photoionization mass spectra in the energy range of the first three carbonyl loss reactions are plotted in Fig. 2. Below 9.7 eV, only the molecular ion, $Cr(CO)_6^+$, and its first CO-loss fragment, $Cr(CO)_5^+$, are present. The $Cr(CO)_6^+$ cation is observed as a symmetric peak at around 33.1 μs, while the $Cr(CO)_5^+$ fragment ion peak is asymmetric and broad with a time-of-flight between 30.7–32.3 μs at low photon energies. The $Cr(CO)_4^+$ and $Cr(CO)_3^+$ cations also show slight asymmetries between 28.5–29.5 μs and 25.9–26.4 μs, respectively. This indicates that the first three carbonyl-loss channels are slow at threshold and their precursor ions are metastable on the time scale of the experiment. The fragment ion peak shapes are indicative of the rate constant and were modeled simultaneously with the breakdown diagram to obtain the experimental unimolecular rate curve and to extrapolate it to threshold, thereby taking the kinetic shift into account.

The best model temperature was found to be 300 K, in agreement with the room temperature experiment. In the SSACM model for the $Cr(CO)_6^+$ CO-loss rate curve, the rigidity constant c was adjusted along with the E_0, in order to reproduce the experimental data. First, using the literature IE of 8.19 ± 0.07 eV, a best fit of $c = 80\ \text{cm}^{-1}$ and $E_0 = 9.625 \pm 0.035$ eV was obtained, which yields a bond dissociation energy of 1.436 ± 0.074 eV – in excellent agreement with the revised BDE[$(CO)_5Cr^+$—CO] = 1.43 ± 0.09 eV of Muntean and Armentrout [13]. Noting that unlike our BDE, the Armentrout et al. value was determined directly, we have then opted to use this BDE and optimized the IE instead to obtain the appearance energy, E_0, resulting in 8.195 ± 0.120 eV, taking the full error bar of the Armentrout BDE into account. This optimized IE value, which is now independent from any PES studies, was used in the rest of the statistical model. 0 K appearance energies of 10.346 ± 0.035 eV and 10.990 ± 0.037 eV were determined for the second and third CO-loss channels, producing $Cr(CO)_4^+$ and $Cr(CO)_3^+$ fragment ions, respectively.

Above 11 eV photon energy, the fragment ion TOF peak shapes are all symmetric, indicating fast dissociation processes and the statistical model is only used to calculate the product energy distribution of the intermediate fragment ions, assuming two translational degrees of freedom [34]. We derived the 0 K appear-

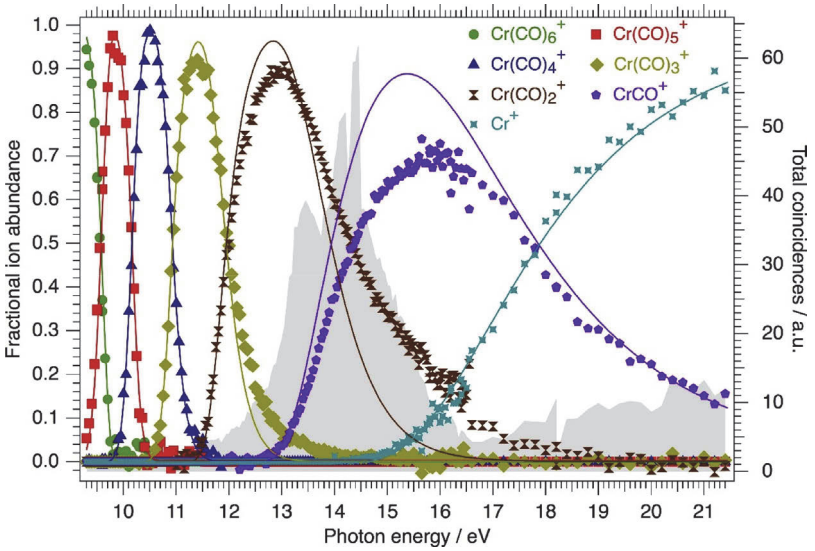

Fig. 1. Breakdown diagram showing the six consecutive CO-losses of $Cr(CO)_6^+$ in the 9.3–21.5 eV photon energy range. Closed polygons are experimentally measured ion abundances, and lines are the best-fit modeling of the data. Gray shadows behind the breakdown curves are representing the absolute threshold photoelectron count, showing the location of the first excited state band of the $Cr(CO)_6^+$ ion.

Table 1
Summary of appearance energies (E_0 / eV) for the sequential CO-loss channels of $Cr(CO)_6^+$.

	This work	Qi et al. [14]	Ng et al. [15]	Meisels et al. [16] [a]	Michels et al. [17] [a]
$Cr(CO)_5^+$	9.625 ± 0.035 [b]	9.29 ± 0.01	9.55 ± 0.04	9.73 ± 0.24	9.85 ± 0.03
$Cr(CO)_4^+$	10.346 ± 0.035	9.85 ± 0.02	10.08 ± 0.04	9.95 ± 0.10	10.45 ± 0.03
$Cr(CO)_3^+$	10.990 ± 0.037	10.62 ± 0.02	10.78 ± 0.09	10.78 ± 0.14	11.35 ± 0.03
$Cr(CO)_2^+$	11.716 ± 0.040	11.27 ± 0.03	11.48 ± 0.11	11.44 ± 0.13	12.51 ± 0.04
$CrCO^+$	12.770 ± 0.060	13.19 ± 0.03	≤ 12.78 ± 0.13	12.80 ± 0.10	14.03 ± 0.04
Cr^+	13.861 ± 0.040	14.12 ± 0.03	< 14.67 ± 0.26	14.13 ± 0.11	15.36 ± 0.03

[a] The authors assumed negligible kinetic energy of the fragmentation products and used their appearance energies to calculate 298 K thermochemistry.
[b] This E_0 was obtained by fixing the BDE to the Armentrout value [13] and optimizing the adiabatic ionization energy.

Table 2
Ionization energy (IE) and 0 K bond dissociation energies (BDE).

	This work	Armentrout et al. [12,13]	Qi et al. [14]	Ng et al. [15]
	IE / eV			
$Cr(CO)_6$	8.195 ± 0.120 [a]	8.19 ± 0.07 [b]	8.10 ± 0.01	8.157 ± 0.026
	BDE / eV			
$(CO)_5Cr–CO^+$	1.43 ± 0.09 [c]	1.43 ± 0.09	1.19 ± 0.02	1.39 ± 0.05
$(CO)_4Cr–CO^+$	0.721 ± 0.049	0.64 ± 0.03	0.56 ± 0.03	0.53 ± 0.6
$(CO)_3Cr–CO^+$	0.644 ± 0.051	0.53 ± 0.08	0.77 ± 0.04	0.70 ± 0.10
$(CO)_2Cr–CO^+$	0.726 ± 0.054	0.56 ± 0.06	0.65 ± 0.05	0.70 ± 0.14
$(CO)Cr–CO^+$	1.054 ± 0.072	0.98 ± 0.03	1.92 ± 0.06	≤ 1.30 ± 0.17
$Cr–CO^+$	1.091 ± 0.072	0.93 ± 0.04	0.93 ± 0.06	> 0.47 ± 0.01 [d]
Sum of BDE	5.666 ± 0.126	5.07 ± 0.15	6.02 ± 0.03 [d]	≤ 6.51 ± 0.26 [e]

[a] Obtained by fixing the first BDE to the Armentrout et al. value and optimizing the IE to the PEPICO data.
[b] The ionization energy is the average of two literature values, see text.
[c] Taken from Armentrout et al. [13].
[d] Estimated lower value from the thermochemical threshold of the ground state Cr^+ formation, 13.26 eV [15].
[e] Calculated here based on the reported IE and $E_0[Cr^+]$.

ance energies as $E_0 = 11.716 \pm 0.040$ eV, 12.770 ± 0.060 eV, and 13.861 ± 0.040 eV, for the $Cr(CO)_2^+$, $CrCO^+$, and Cr^+ fragment ions, respectively (see Table 1).

While the breakdown diagram is very well reproduced up to the crossover energy of $Cr(CO)_3^+$ and $Cr(CO)_2^+$ at roughly 12 eV, the statistical model and the experimental data diverge in the intermediate energy range between 12–16 eV. On the one hand, this is not entirely unexpected, since the calculated dissociation rates for the first CO-loss step are larger than 10^{16} s^{-1} at a parent ion internal energy of 6.8 eV (15 eV photon energy). Even if this is a significant overestimation, there may be insufficient time for the system to explore the phase space prior to dissociation and the ergodic hypothesis may not hold. On the other hand, the agreement between the model and the experimental breakdown diagram is restored at photon energies above 17 eV, which suggests a more specific and transient reason for the non-statistical fragmentation mechanism at intermediate energies. A clue is provided by the photoelectron spectrum, in which the photoelectron band in the 12–16.5 eV range is indeed separated from the ground state band at 8–9.5 eV by a substantial Franck–Condon gap [47]. Therefore, the coupling between the ground and the excited state may be weak and the excited state lifetime long, which was shown to be accountable for the existence of two, otherwise statistical, but de-coupled fragmentation regimes of the tetrafluoroethylene cation [48].

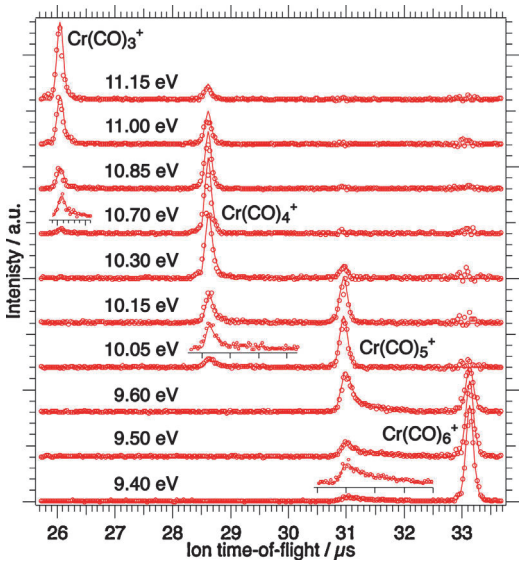

Fig. 2. Sample threshold photoionization TOF distributions. Open circles are the experimentally measured PEPICO mass spectra and lines are the best fit modeling of the data.

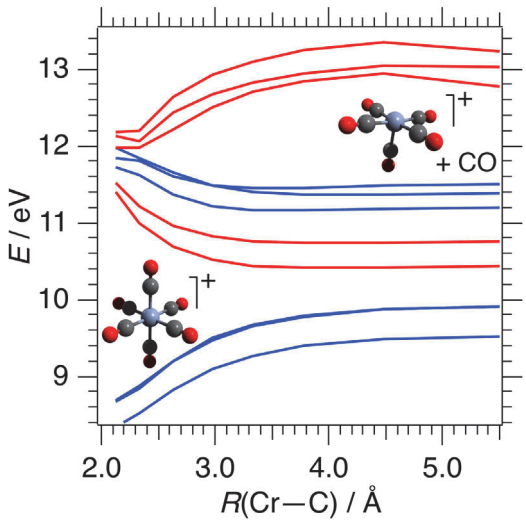

Fig. 3. (TD-)DFT CO-loss potential energy curves relative to the neutral $Cr(CO)_6$ minimum, calculated using B3LYP/6-311++G(d,p) along optimized CO-loss geometries on the ground electronic state of $Cr(CO)_6^+$. Blue curves correspond to doublet, red curves to quartet states (For interpretation of the references to colour in this figure legend, the reader is referred to the web version of this article).

Dissociation reactions on repulsive electronic states entail suprastatistical kinetic energy release and a smaller fraction of the excess internal energy is retained in the fragment ion. Therefore, less energy is made available for the sequential dissociations and the statistical model should overestimate the degree of fragmentation in the non-statistical energy range. It is nonetheless surprising that the breakdown diagram is well reproduced by the statistical model at higher energies. However, both CCl_4 and SF_5CF_3 have been shown to photoionize dissociatively and impulsively in the ground electronic state but statistically at higher energies [49,50]. This means that a return to statisticality is possible at higher energies, even if a repulsive state lies below. Yet $Cr(CO)_6^+$ is, to the best of our knowledge, the first system in which a non-statistical episode is found to be bracketed by statistical fragmentation both at low and at high energies.

The candidate for non-statistical dissociation most affecting the breakdown diagram is CO-loss from the molecular ion $Cr(CO)_6^+$, because most excess energy is available in this step and a significant amount may be lost in translation. Therefore, we have examined the electronic structure of $Cr(CO)_6^+$ along the CO-loss coordinate using time-dependent density functional theory for the excited states, as plotted in Fig. 3. Reaction energy curves along the optimized CO-loss coordinate in the cation ground state, calculated at the M06-2X/def2-TZVPP and B3LYP/6-311++G(d,p) levels of theory, as well as two EOM-EE-CCSD/cc-pVDZ calculations at the equilibrium and elongated Cr—C bond lengths using the Q-Chem 4.3 program package [38] confirmed the results shown in Fig. 3. The lowest electronic states of the cation, corresponding to Cr $3d^{-1}$ ionization, are bound with respect to CO loss. However, all doublet and some quartet states, computed to lie in the second photoelectron band of $Cr(CO)_6$, are repulsive. Furthermore, even at higher energies, direct ionization yields a doublet and an intersystem crossing (ISC) is required to reach a bound quartet surface, which may be too slow and not compete effectively with impulsive CO loss on the doublet surface. The fact that CO loss from $Cr(CO)_6^+$ in the energy range of the second photoelectron band takes place along a repulsive energy curve explains the enhanced kinetic energy release and internal energy loss, which leads to less fragmentation than predicted by the statistical model.

We have also calculated the excited state CO-loss reaction energy curves in $Cr(CO)_5^+$ and found that the first ten states are all bound, which means that the suppressed fragmentation in the breakdown diagram is entirely due to enhanced kinetic energy release in the first dissociation step. At even higher energies, there may be electronic states that couple more strongly with the ground state, which could be responsible for the return to statisticality. Alternatively, and perhaps more likely, the first dissociation step may take place statistically along an excited quartet potential energy curve after ISC, which is sufficiently long-lived and couples weakly with the impulsive doublet states below. This would suppress the kinetic energy release in the first step, but lead to more energetic intermediate fragment ions, which may then lose more of their internal energy in subsequent CO-loss steps. These two effects may cancel each other out, yielding a statistical fragment ion energy distribution.

The statistical model provided appearance energies of 12.770 ± 0.060 eV, and 13.861 ± 0.040 eV for the $CrCO^+$ and Cr^+ ions, respectively; however, because of the disagreement between the experimental breakdown curve for $CrCO^+$ and the statistical model, we need to examine the reliability of these values. At these photon energies, the width of the initial thermal energy distribution is negligible compared to the excess photon energy above the IE and the breakdown curves reflect how much of the excess energy is lost into translation and CO rotation/vibration in each dissociation step. Thus, the rising edge of a daughter ion breakdown curve corresponds to the ion population that have lost the least possible excess energy and these parts of the breakdown curves, the rising edges, are least affected by impulsive dissociation. The fact that even the problematic $CrCO^+$ breakdown curve is reproduced well up to 0.5 eV above its appearance tells us that its derived appearance energy should be reliable. Furthermore, the fact that the entire Cr^+ breakdown curve is well reproduced statistically tells us that the internal energy distribution of its parent, the $CrCO^+$ fragment ion, is very well described in this photon energy range by the statistical model and the derived appearance energy is very likely correct.

3.2. *Appearance energies, bond dissociation energies, and thermochemistry*

The appearance energies derived in this work are summarized and compared to earlier studies in Table 1. Rather scattered onsets

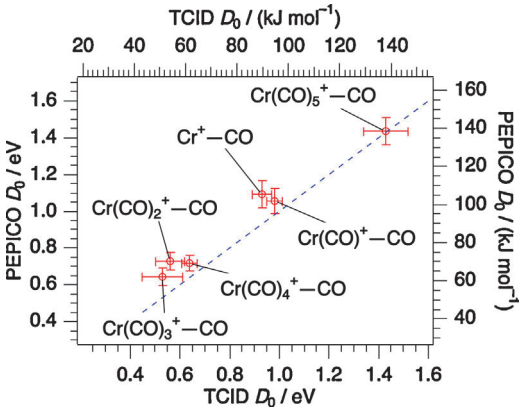

Fig. 4. Comparison of PEPICO (this work) and TCID (Armentrout et al. [12,13]) $[(CO)_nCr{-}CO]^+$, n = 0–5, bond dissociation energies. Note that, for comparison, the first BDE$[(CO)_5Cr^+{-}CO]$ used for this Figure (and not for the thermochemistry, *vide infra*) is obtained by using Armentrout's IE and depends on the choice of IE. It shows, however, very good agreement with the TCID value, which is independent of the IE. The other five Cr–CO ionic bond energies show a qualitative agreement, but the TCID data is systematically lower by 0.12 ± 0.04 eV than the PEPICO values.

were reported in earlier photoionization experiments, and the appearance energy of the Cr^+ fragment ion is, in particular, significantly higher in every photoionization study compared to the TCID experiment.

We also calculated ionic bond dissociation energies using the six appearance energies (E_0 for $Cr(CO)_n^+$; n = 5–0 as listed in Table 1). The BDE were also reported by Qi et al. [14] and Ng et al. [15] in their photoionization studies but they were measured directly by Armentrout et al. [12,13] using TCID.

As noted above, the first BDE was fixed at 1.43 ± 0.09 eV as the TCID determination of this quantity does not rely on the choice of the IE. [13] The other five Cr—CO ionic bond energies show a very good qualitative agreement between the PEPICO and TCID data but the latter are systematically lower by 0.12 ± 0.04 eV than the PEPICO values, as depicted in Fig. 4. These values can also be compared to some literature determinations. Barnes et al. [5] used SCF/MCPF calculations with ECP basis set on the Cr to obtain the BDE of $(CO)Cr^+{-}CO$ and $Cr^+{-}CO$ which, perchance, happen to coincide with Armentrout's values. The reliability of such calculations, however, is questionable because an exact *ab initio* treatment of these systems is prohibitively expensive, as it has to involve relativistic, spin–orbit, and non-Born–Oppenheimer effects. DFT calculations, on the other hand, rely on semiempirical parametrization, which may be less dependable without converged wave function theory or reliably established experimental data points.

It is clear from Fig. 4 that the largest BDE is of $(CO)_5Cr{-}CO^+$, somewhat lower bond energies are found for $(CO)Cr{-}CO^+$ and $Cr{-}CO^+$, and the weakest Cr—CO bonds are found in $(CO)_4Cr{-}CO^+$, $(CO)_3Cr{-}CO^+$, and $(CO)_2Cr{-}CO^+$. As discussed at length by Armentrout et al. [12], a significant driving force behind the varying bond energies is the change in spin multiplicity. Considering the bond energies all in the doublet state, the appearance energy of Cr^+ should be around 17 eV. However, compared to the parent ion, the smaller ions become progressively more stable in quartet or sextet states, effectively lowering the bond dissociation energy upon spin change.

3.3. Thermochemistry

The neutral $Cr(CO)_6$ molecule or the final product Cr^+ ion could both be used as the thermochemical anchor to derive heats of formation from the PEPICO bond dissociation energies. The enthalpy of formation of Cr^+ is certainly well established at

Table 3
Auxiliary and derived thermochemical data (kJ mol^{-1}).

Species	$\Delta_fH_{0\,K}$	$\Delta_fH_{298\,K}$	Error	$H_{298K} - H_{0K}$[a]
Cr^+	1048.14[b]	1050.28[b]	± 1.50	
$CrCO^+$	829.1[c]	830.9[c,d]	± 7.1	11.25
$Cr(CO)_2^+$	613.6[c]	616.1[c,d]	± 5.7	17.37
$Cr(CO)_3^+$	429.7[c]	432.9[c,d]	± 5.5	23.45
$Cr(CO)_4^+$	253.8[c]	258.4[c,d]	± 5.3	30.28
$Cr(CO)_5^+$	70.4[c]	76.4[c,d]	± 5.3	37.02
$Cr(CO)_6^+$	−181.4[c]	−176.7[c,d]	± 12.3	41.08
	−121.8[e]	−117.1[e]	± 7.1	
$Cr(CO)_6$ (g)	−972.1[c]	−968.9[c,d]	± 4.1	39.58
	−912.1[e]	−908.3[e]	± 1.7	
$Cr(CO)_6$ (s)		−1040.6[c]	± 4.2	
		−932.6[f]	± 2.1	
		−980.3[f]	± 1.7	
		−978.2[g]	± 18.8	
		−979.9[g]	± 2.3	
		−999.6[g]	± 1.7	
		−982.2[h]	± 4.6	
		−1043.5[i]		
		−1077.8[j]		
CO	−113.803[k]	−110.523[k]	± 0.026	

[a] Based on B3LYP/6-311++G(d,p) vibrational frequencies.
[b] NIST-JANAF Thermochemical Tables [51].
[c] This work (see Table 1).
[d] Converted to T = 298 K using harmonic vibrational frequencies and known elemental thermal enthalpies [51].
[e] Armentrout et al., converted to the Rosenstock (ion) convention [12].
[f] Connor et al. [52].
[g] Pittam et al. [22].
[h] Sheiman et al. [56].
[i] Sharifov and Rezukhina [54] originally published −1078.6 kJ mol^{-1}, which was critically reviewed and corrected based on revised ancillary data by Cotton et al. [55] to −1043.5 kJ mol^{-1}. Cotton et al. later reports [22] this revised value, albeit they report the author names as Sharafov and Rezukhina, a likely mistransliteration.
[j] Cotton et al. [55].
[k] Active Thermochemical Tables (ATcT) [57].

$\Delta_fH_{0K}(Cr^+)$ = 1048.14 ± 1.5 kJ mol^{-1} [51]. However, we argue that this is not the case for $Cr(CO)_6$, contrary to what the 1975 paper by Pittam et al. asserts [22]. Here, the 298 K enthalpy of formation of solid $Cr(CO)_6$ was reported as $\Delta_fH_{298\,K}[Cr(CO)_6, c]$ = −979.9 ± 1.7 kJ mol^{-1}, calculated as a weighted mean value of three different calorimetric measurements [22]. By selecting the three values that agree well, they neglected the fact that there are several other calorimetric measurements, two of them in fact reported as alternative values in the same papers the three selected values stemmed from (combustion *vs.* thermal decomposition and thermal decomposition *vs.* iodination), which put the solid $Cr(CO)_6$ heat of formation between −1077.8 and −932.6 kJ mol^{-1}, spanning a rather impressive range of almost 150 kJ mol^{-1}. Interestingly, each of these values were reported with enviably low (typically <5 kJ mol^{-1}) and, therefore, dubious error bars, which likely corresponded to random errors in the measurement only, overlooking much larger systematic errors and their effects on the uncertainty. The alternative values from Connor et al. [52] and Pittam et al. [22] also differ by 67 kJ mol^{-1} from each other, putting the supposedly consensus value into a vastly different light. After a review of the calorimetric literature, one cannot help but conclude that the solid $Cr(CO)_6$ heat of formation is anything but settled.

Therefore, in our thermochemical calculations, we have derived the enthalpies of formation of the $Cr(CO)_n^+$ ions, n = 0–6, and of gas-phase $Cr(CO)_6$ neutral from the Cr^+ anchor, with the help of ancillary thermochemical data, as summarized in Table 3 and briefly outlined here. The 0 K heat of formation of $CrCO^+$ is calculated as:

$$\Delta_fH_{0K}[CrCO^+] = \Delta_fH_{0K}[Cr^+] + \Delta_fH_{0K}[CO] - (E_0[Cr^+] - E_0[CrCO^+])$$

Similarly, the heats of formation of $Cr(CO)_n^+$ ($2 \le n \le 5$) can be obtained from the Cr^+ and CO heats of formation and the appearance energy difference between Cr^+ and $Cr(CO)_n^+$. For the $Cr(CO)_6^+$ molecular ion, the adiabatic ionization energy of $Cr(CO)_6$ is used instead of the appearance energy as:

$$\Delta_f H_{0K}[Cr(CO)_6^+] = \Delta_f H_{0K}[Cr^+] + 6\ \Delta_f H_{0K}[CO] - (E_0[Cr^+] - IE[Cr(CO)_6])$$

And, finally, for the precursor neutral compound, $Cr(CO)_6$ (g), the heat of formation is calculated simply from the 0 K appearance energy of the Cr^+ ion:

$$\Delta_f H_{0K}[Cr(CO)_6, g] = \Delta_f H_{0K}[Cr^+] + 6\ \Delta_f H_{0K}[CO] - E_0[Cr^+]$$

To obtain the 298 K heat of formation of the gaseous ions and neutrals discussed above, we used the known elemental thermal enthalpies [51] and B3LYP/6-311++G(d,p) calculated thermal enthalpies to convert the 0 K heats of formation to 298 K. Room temperature values for cations are listed according to the ion or Rosenstock convention [53] in Table 3. For the $Cr(CO)_6$ parent molecule, this gave a heat of formation of $\Delta_f H_{298\,K}[Cr(CO)_6$ (g)] = -968.9 ± 3.9 kJ mol^{-1}. Since the 298 K heat of sublimation for $Cr(CO)_6$ was measured by Pilcher et al. [22] as 71.7 ± 0.4 kJ mol^{-1}, we can also derive the 298 K heat of formation for crystalline $Cr(CO)_6$ as $\Delta_f H_{298\,K}[Cr(CO)_6$, c] = -1040.6 ± 4.2 kJ mol^{-1}. This is more than 60 kJ mol^{-1} lower than the Pittam et al. recommended value, but shows serendipitous agreement with $\Delta_f H_{298\,K}[Cr(CO)_6$, c] = -1043.5 ± 1.7 kJ mol^{-1} reported in an even earlier calorimetric study by Sharifov and Rezukhina in 1953 [54], as revised by Cotton et al. (see also the footnote in Table 3) [55].

Such a large correction over a decades old, seemingly well-established thermochemical value certainly requires some justification and it is important to note that our derived heat of formation of $Cr(CO)_6$ only depends on the Cr^+ and CO heats of formation, both well established; the Pilcher heat of sublimation, and just one PEPICO appearance energy: $E_0(Cr^+)$. However, the statistical model that we used to derive this latter value also depends somewhat on the other appearance energies (or bond dissociation energies) as the five product energy distribution calculations in the model are a function of the excess internal energy above the respective dissociation thresholds. Therefore, we have also carried out a complete modeling using the Armentrout TCID bond dissociation energies either by fixing all or only the first five BDE at the TCID values and fitting none or only the last one. The calculated breakdown curves from these models are shown in Figure S1 in the Supporting Information (SI). The optimized appearance energy of the Cr^+ ion is 13.694 eV in this model (dotted Cr^+ breakdown curve in Figure S1), which is still within 170 meV (16 kJ mol^{-1}) of our best-fit value. More importantly, it is immediately obvious that there is a systematically increasing redshift of the breakdown curves with increasing fragmentation, which is clearly inconsistent with the experimental data and suggests that the TCID bond energies are systematically underestimated. Therefore, we suggest that the agreement between the TCID bond energy sum with Pittam's calorimetry value for the $Cr(CO)_6$ heat of formation is accidental and the newly derived value based on the Cr^+ anchor and the PEPICO appearance energy of Cr^+ is the most reliable value for this key transition metal carbonyl.

4. Conclusions

The unimolecular dissociation of internal energy selected chromium hexacarbonyl cations was investigated by imaging Photoelectron Photoion Coincidence Spectroscopy using VUV synchrotron radiation from the Swiss Light Source. $Cr(CO)_6^+$ dissociates by consecutively losing all six carbonyl ligands in the 9.3 to 21.5 eV photon energy range. The first three CO-loss reactions are slow on the time scale of the experiment. Hence, we modeled the time-of-flight mass spectra along with the fractional ion abundances, plotted in the breakdown diagram, to determine accurate dissociation onsets. Measured unimolecular dissociation rates were fitted using the simplified statistical adiabatic channel model (SSACM) and extrapolated to the threshold, yielding a 0 K appearance energy of 9.625 ± 0.035 eV for the first CO loss. This value was obtained by accepting the TCID C–Cr bond dissociation energy in $Cr(CO)_6^+$ and optimizing the ionization energy of $Cr(CO)_6$, which yielded IE = 8.195 ± 0.120 eV, a value independent on the intuition-based assignment of the unresolved group state photoelectron band. We also derived the 0 K dissociation onsets of 10.346 ± 0.035 eV, 10.990 ± 0.037 eV, 11.716 ± 0.040 eV, 12.770 ± 0.060 eV, and 13.861 ± 0.040 eV for the $Cr(CO)_4^+$, $Cr(CO)_3^+$, $Cr(CO)_2^+$, $CrCO^+$, and Cr^+ fragment ions, respectively. These results may also serve as valuable benchmarks for organometallic compounds, which are notoriously hard to calculate.

Comparing the experimental and modeled breakdown curves, we have also discovered a unique feature of the dissociation mechanism: at intermediate internal energies, a non-statistical episode is bracketed by statistical fragmentation both at low and at high energies. As confirmed by TD-DFT calculations, this is brought about by repulsive doublet states of the parent ion in the energy range of the second photoelectron band. Excitation to these doublet states leads to enhanced kinetic energy release and, consequently, suppressed degree of fragmentation. At higher energies, the statistical model fits the experimental data quite well, which suggests a return to statisticality, as other bound states are formed, which couple weakly with the repulsive electronic states in the parent ion. To the best of our knowledge, this is the first system for which such an observation has been reported.

Although the bond dissociation energies follow the trend of the earlier TCID measurements [12,13], they are systematically higher than these. Since the literature enthalpies of formation of $Cr(CO)_6$ (g) and Cr^+ are connected directly by the Cr^+ appearance energy in our photoionization experiment, our disagreement with both the literature thermochemistry and TCID data hints at several possible sources of error. If we convert the TCID bond energies to appearance energies, the discrepancy with the breakdown diagram is large already in the second step, and gets progressively larger as the fragmentation progresses, which indicates that the binding energies have been consistently underestimated and these, individually small, errors are amplified in their sum. Furthermore, the literature $\Delta_f H_{298K}[Cr(CO)_6$, g] is based on an expectedly trustworthy sublimation enthalpy but a rather dubious averaging of a select few calorimetry experiments, disregarding the majority of calorimetry results without cause. We, therefore, use the Cr^+ appearance energy together with well-defined ancillary thermochemical data to report a revised chromium hexacarbonyl heat of formation, both in the gas and the crystalline phases.

Acknowledgements

This work has been funded by the National Science Foundation (Grant No. CHE-1665464) and by the Swiss Federal Office for Energy (BFE Contract No. SI/501269-01). J.P.K. acknowledges the Hiram College Chemistry Department, Dean's Office, and the ACS PRF (51896-UNI4) for financial support. The iPEPICO experiments were performed at the VUV beamline of the Swiss Light Source (Paul Scherrer Institut, Villigen, Switzerland).

Appendix A. Supplementary data

Supplementary material related to this article can be found, in the online version, at doi:https://doi.org/10.1016/j.ijms.2018.12.010.

References

[1] E.W. Plummer, W.R. Salaneck, J.S. Miller, Photoelectron spectra of transition-metal carbonyl complexes: comparison with the spectra of adsorbed CO, Phys. Rev. B 18 (1978) 1673–1701, http://dx.doi.org/10.1103/PhysRevB.18.1673.

[2] M. Wrighton, Photochemistry of metal carbonyls, Chem. Rev. 74 (1974) 401–430, http://dx.doi.org/10.1021/cr60290a001.

[3] M. Zhou, L. Andrews, C.W. Bauschlicher, Spectroscopic and theoretical investigations of vibrational frequencies in binary unsaturated transition-metal carbonyl cations, neutrals, and anions, Chem. Rev. 101 (2001) 1931–1962, http://dx.doi.org/10.1021/cr990102b.

[4] D. Astruc, Organometallic Chemistry and Catalysis, Vol. 291, Springer, Heidelberg, 2007, pp. 608, http://dx.doi.org/10.1007/978-3-540-46129-6.

[5] L.A. Barnes, M. Rosi, C.W. Bauschlicher, Theoretical studies of the first- and second-row transition-metal mono- and dicarbonyl positive ions, J. Chem. Phys. 93 (1990) 609–624, http://dx.doi.org/10.1063/1.459508.

[6] A.W. Ehlers, G. Frenking, Structures and bond energies of the transition metal hexacarbonyls $M(CO)_6$ (M = Cr, Mo, W). A theoretical study, J. Am. Chem. Soc. 116 (1994) 1514–1520, http://dx.doi.org/10.1021/ja00083a040.

[7] L.A. Barnes, B. Liu, R. Lindh, Structure and energetics of $Cr(CO)_6$ and $Cr(CO)_5$, J. Chem. Phys. 98 (1993) 3978–3989, http://dx.doi.org/10.1063/1.464026.

[8] S. Dapprich, U. Pidun, A.W. Ehlers, G. Frenking, The calculation of bond dissociation energies of transition metal complexes using isostructural reactions, Chem. Phys. Lett. 242 (1995) 521–526, http://dx.doi.org/10.1016/0009-2614(95)00759-W.

[9] J. Kim, T.K. Kim, J. Kim, Y.S. Lee, H. Ihee, Density functional and ab initio study of $Cr(CO)_n$ (n = 1–6) complexes, J. Phys. Chem. A 111 (2007) 4697–4710, http://dx.doi.org/10.1021/jp066081o.

[10] L. Andrews, M. Zhou, G.L. Gutsev, X. Wang, Reactions of laser-ablated chromium atoms, cations, and electrons with CO in excess argon and neon: infrared spectra and density functional calculations on neutral and charged unsaturated chromium carbonyls, J. Phys. Chem. A 107 (2003) 561–569, http://dx.doi.org/10.1021/jp026955g.

[11] E. Martínez-Núñez, A. Fernández-Ramos, S.A. Vázquez, J.M.C. Marques, M. Xue, W.L. Hase, Quasiclassical dynamics simulation of the collision-induced dissociation of $Cr(CO)_6^+$ with Xe, J. Chem. Phys. 123 (2005), 154311, http://dx.doi.org/10.1063/1.2044687.

[12] F.A. Khan, D.E. Clemmer, R.H. Schultz, P.B. Armentrout, Sequential bond energies of chromium carbonyls $(Cr(CO)_x^+$, x = 1–6), J. Phys. Chem. 97 (1993) 7978–7987, http://dx.doi.org/10.1021/j100132a029.

[13] F. Muntean, P.B. Armentrout, Guided ion beam study of collision-induced dissociation dynamics: integral and differential cross sections, J. Chem. Phys. 115 (2001) 1213–1228, http://dx.doi.org/10.1063/1.1371958.

[14] F. Qi, X. Yang, S. Yang, H. Gao, L. Sheng, Y. Zhang, S. Yu, Mass resolved photoionization/fragmentation studies of $Cr(CO)_6$ at photon energies of ~8–40 eV, J. Chem. Phys. 107 (1997) 4911–4918, http://dx.doi.org/10.1063/1.474854.

[15] Y.J. Chen, C.L. Liao, C.Y. Ng, A molecular beam photoionization mass spectrometric study of $Cr(CO)_6$, $Mo(CO)_6$, and $W(CO)_6$, J. Chem. Phys. 107 (1997) 4527–4536, http://dx.doi.org/10.1063/1.474814.

[16] P.R. Das, T. Nishimura, G.G. Meisels, Fragmentation of energy-selected hexacarbonylchromium ion, J. Phys. Chem. 89 (1985) 2808–2812, http://dx.doi.org/10.1021/j100259a021.

[17] G.D. Michels, G.D. Flesch, H.J. Svec, Comparative mass spectrometry of the Group 6B hexacarbonyls and pentacarbonyl thiocarbonyls, Inorg. Chem. 19 (1980) 479–485, http://dx.doi.org/10.1021/ic50204a039.

[18] D.R. Bidinosti, N.S. McIntyre, Electron-impact study of some binary metal carbonyls, Can. J. Chem. 45 (1967) 641–648, http://dx.doi.org/10.1139/v67-105.

[19] A. Foffani, S. Pignataro, B. Cantone, F. Grasso, Mass spectra of metal hexacarbonyls, Z. Phys. Chem. 45 (1965) 79–88, http://dx.doi.org/10.1524/zpch.1965.45.1_2.079.

[20] R.E. Winters, R.W. Kiser, Mass spectrometric studies of chromium, molybdenum, and tungsten hexacarbonyls, Inorg. Chem. 4 (1965) 157–161, http://dx.doi.org/10.1021/ic50024a006.

[21] K.E. Lewis, D.M. Golden, G.P. Smith, Organometallic bond dissociation energies: laser pyrolysis of iron pentacarbonyl, chromium hexacarbonyl, molybdenum hexacarbonyl, and tungsten hexacarbonyl, J. Am. Chem. Soc. 106 (1984) 3905–3912, http://dx.doi.org/10.1103/PhysRevB.18.1673.

[22] D.A. Pittam, G. Pilcher, D.S. Barnes, H.A. Skinner, D. Todd, The enthalpy of formation of chromium hexacarbonyl, J. Less Common Met. 42 (1975) 217–222, http://dx.doi.org/10.1016/0022-5088(75)90007-7.

[23] E.M. Russell, E. Cudjoe, M.E. Mastromatteo, J.P. Kercher, B. Sztáray, A. Bodi, From iron pentacarbonyl to the iron ion by imaging photoelectron photoion coincidence, J. Phys. Chem. A 117 (2013) 4556–4563, http://dx.doi.org/10.1021/jp402443e.

[24] Á. Révész, C.I. Pongor, A. Bodi, B. Sztáray, T. Baer, Manganese–chalcocarbonyl bond strengths from threshold photoelectron photoion coincidence spectroscopy, Organometallics 25 (2006) 6061–6067, http://dx.doi.org/10.1021/om060379j.

[25] C.I. Pongor, L. Szepes, R. Basi, A. Bodi, B. Sztáray, Metal–carbonyl bond energies in phosphine analogue complexes of $Co(CO)_3NO$ by photoelectron photoion coincidence spectroscopy, Organometallics 31 (2012) 3620–3627, http://dx.doi.org/10.1021/om300132g.

[26] X.-G. Zhang, P.B. Armentrout, Sequential bond energies of $Pt(CO)_x^+$ (x= 1– 4) determined by collision-induced dissociation, Organometallics 20 (2001) 4266–4273, http://dx.doi.org/10.1021/om010390d.

[27] P.B. Armentrout, Activation of C_2H_6 and C_3H_8 by gas-phase Mo^+: thermochemistry of Mo–ligand complexes, Organometallics 26 (2007) 5473–5485, http://dx.doi.org/10.1021/om700579m.

[28] Z. Gengeliczki, B. Sztáray, T. Baer, C. Iceman, P.B. Armentrout, Heats of formation of $Co(CO)_2NOPR_3$, R = CH_3 and C_2H_5, and its ionic fragments, J. Am. Chem. Soc. 127 (2005) 9393–9402, http://dx.doi.org/10.1021/ja0504744.

[29] T. Baer, R.P. Tuckett, Advances in threshold photoelectron spectroscopy (TPES) and threshold photoelectron photoion coincidence (TPEPICO), Phys. Chem. Chem. Phys. 19 (2017) 9698–9723, http://dx.doi.org/10.1039/C7CP00144D.

[30] Y. Li, B. Sztáray, T. Baer, The dissociation kinetics of energy-selected $CpMn(CO)_3^+$ ions studied by threshold photoelectron–photoion coincidence spectroscopy, J. Am. Chem. Soc. 123 (2001) 9388–9396, http://dx.doi.org/10.1021/ja004019d.

[31] A. Bodi, M. Johnson, T. Gerber, Z. Gengeliczki, B. Sztáray, T. Baer, Imaging photoelectron photoion coincidence spectroscopy with velocity focusing electron optics, Rev. Sci. Instrum. 80 (2009), http://dx.doi.org/10.1063/1.3082016, 034101/034101–034101/034107.

[32] M. Johnson, A. Bodi, L. Schulz, T. Gerber, Vacuum ultraviolet beamline at the Swiss Light Source for chemical dynamics studies, Nucl. Instrum. Methods Phys. Res. A 610 (2009) 597–603, http://dx.doi.org/10.1016/j.nima.2009.08.069.

[33] W.C. Wiley, I.H. McLaren, Time-of-flight mass spectrometer with improved resolution, Rev. Sci. Instrum. 26 (1955) 1150–1157, http://dx.doi.org/10.1063/1.1715212.

[34] B. Sztáray, A. Bodi, T. Baer, Modeling unimolecular reactions in photoelectron photoion coincidence experiments, J. Mass Spectrom. 45 (2010) 1233–1245, http://dx.doi.org/10.1002/jms.1813.

[35] A. Bodi, B. Sztáray, T. Baer, M. Johnson, T. Gerber, Data acquisition schemes for continuous two-particle time-of-flight coincidence experiments, Rev. Sci. Instrum. 78 (2007), 084102, http://dx.doi.org/10.1063/1.2776012.

[36] B. Sztáray, T. Baer, Suppression of hot electrons in threshold photoelectron photoion coincidence spectroscopy using velocity focusing optics, Rev. Sci. Instrum. 74 (2003) 3763–3768, http://dx.doi.org/10.1063/1.1593788.

[37] M.J. Frisch, G.W. Trucks, H.B. Schlegel, G.E. Scuseria, M.A. Robb, J.R. Cheeseman, G. Scalmani, V. Barone, B. Mennucci, G.A. Petersson, H. Nakatsuji, M. Caricato, X. Li, H.P. Hratchian, A.F. Izmaylov, J. Bloino, G. Zheng, J.L. Sonnenberg, M. Hada, M. Ehara, K. Toyota, R. Fukuda, J. Hasegawa, M. Ishida, T. Nakajima, Y. Honda, O. Kitao, H. Nakai, T. Vreven, J.A. Montgomery Jr., J.E. Peralta, F. Ogliaro, M. Bearpark, J.J. Heyd, E. Brothers, K.N. Kudin, V.N. Staroverov, R. Kobayashi, J. Normand, K. Raghavachari, A. Rendell, J.C. Burant, S.S. Iyengar, J. Tomasi, M. Cossi, N. Rega, J.M. Millam, M. Klene, J.E. Knox, J.B. Cross, V. Bakken, C. Adamo, J. Jaramillo, R. Gomperts, R.E. Stratmann, O. Yazyev, A.J. Austin, R. Cammi, C. Pomelli, J.W. Ochterski, R.L. Martin, K. Morokuma, V.G. Zakrzewski, G.A. Voth, P. Salvador, J.J. Dannenberg, S. Dapprich, A.D. Daniels, Ö. Farkas, J.B. Foresman, J.V. Ortiz, J. Cioslowski, D.J. Fox, Gaussian 09, Gaussian, Inc, Wallingford, CT, 2009.

[38] Y. Shao, Z. Gan, E. Epifanovsky, A.T.B. Gilbert, M. Wormit, J. Kussmann, A.W. Lange, A. Behn, J. Deng, X. Feng, Advances in molecular quantum chemistry contained in the Q-Chem 4 program package, Mol. Phys. 113 (2015) 184–215, http://dx.doi.org/10.1080/00268976.2014.952696.

[39] T. Baer, W.L. Hase, Unimolecular Reaction Dynamics: Theory and Experiments; Oxford University Press on Demand, 1996, pp. 448, ISBN: 0195074947.

[40] T. Beyer, D.F. Swinehart, Algorithm 448: number of multiply-restricted partitions, Commun. ACM 16 (1973) 379, http://dx.doi.org/10.1145/362248.362275.

[41] W. Stevens, B. Sztáray, N. Shuman, T. Baer, J. Troe, Specific rate constants k(E) of the dissociation of the halobenzene ions: analysis by statistical unimolecular rate theories, J. Phys. Chem. A 113 (2008) 573–582, http://dx.doi.org/10.1021/jp807930k.

[42] G.A. Junk, H.J. Svec, Energetics of the ionization and dissociation of $Ni(CO)_4$, $Fe(CO)_5$, $Cr(CO)_6$, $Mo(CO)_6$ and $W(CO)_6$, Z. Naturforsch. B 23 (1968) 1–9, http://dx.doi.org/10.1515/znb-1968-0102.

[43] D.R. Lloyd, E.W. Schlag, Photoionization studies of metal carbonyls. I. Ionization potentials and the bonding in Group VI metal hexacarbonyls and in mononuclear carbonyls and nitrosyl carbonyls of iron, cobalt, and nickel, Inorg. Chem. 8 (1969) 2544–2555, http://dx.doi.org/10.1021/ic50082a003.

[44] J.L. Hubbard, D.L. Lichtenberger, Vibrational fine structure in the valence ionizations of transition metal hexacarbonyls: new experimental indication of metal-to-carbonyl π bonding, J. Am. Chem. Soc. 104 (1982) 2132–2138, http://dx.doi.org/10.1021/ja00372a008.

[45] S.G. Lias, J.E. Bartmess, J.F. Liebman, J.L. Holmes, R.D. Levin, W.G. Mallard, Gas-phase ion and neutral thermochemistry, J. Phys. Chem. Ref. Data 17 (Supplement No. 1) (1988) 1–861, ISBN: 0883185628.

[46] M.F. Heringa, J.G. Slowik, A.S.H. Prévôt, U. Baltensperger, P. Hemberger, A. Bodi, Dissociative ionization mechanism and appearance energies in adipic acid revealed by imaging photoelectron photoion coincidence, selective deuteration, and calculations, J. Phys. Chem. A 120 (2016) 3397–3405, http://dx.doi.org/10.1021/acs.jpca.6b00908.
[47] G. Cooper, J.C. Green, M.P. Payne, B.R. Dobson, I.H. Hillier, Photoelectron spectroscopy with variable photon energy. A study of the metal hexacarbonyls $M(CO)_6$ where M = Cr, Mo, and W, J. Am. Chem. Soc. 109 (1987) 3836–3843, http://dx.doi.org/10.1021/ja00247a003.
[48] J. Harvey, A. Bodi, R.P. Tuckett, B. Sztáray, Dissociation dynamics of fluorinated ethene cations: from time bombs on a molecular level to double-regime dissociators, Phys. Chem. Chem. Phys. 14 (2012) 3935–3948, http://dx.doi.org/10.1039/C2CP23878K.
[49] J. Harvey, R.P. Tuckett, A. Bodi, Shining new light on the multifaceted dissociative photoionisation dynamics of CCl_4, Phys. Chem. Chem. Phys. 16 (2014) 20492–20499, http://dx.doi.org/10.1039/c4cp03009e.
[50] A. Bodi, P. Hemberger, R.P. Tuckett, Coincident velocity map image reconstruction illustrated by the single-photon valence photoionisation of CF_3SF_5, Phys. Chem. Chem. Phys. 19 (2017) 30173–30180, http://dx.doi.org/10.1039/C7CP05576E.
[51] M.W. Chase, C.A. Davies Jr, NIST-JANAF Thermochemical Tables, 4th edn, American Institute of Physics for the National Institute of Standards and Technology, New York, 1998, pp. 1963, ISBN: 1-56396-831-2.
[52] J.A. Connor, H.A. Skinner, Y. Virmani, Microcalorimetric studies. Thermal decomposition and iodination of metal carbonyls, J. Chem. Soc. Faraday Trans. 68 (1972) 1754–1763, http://dx.doi.org/10.1039/F19726801754.
[53] L.G. Christophorou, E. Illenberger, W.F. Schmidt, Linking the gaseous and condensed phases of matter: the behavior of slow electrons, Springer Sci. Bus. Media 326 (2012) 596, http://dx.doi.org/10.1007/978-1-4615-2540-0.
[54] K.A. Sharifov, T.N. Rezukhina, Heats of combustion and heats of formation of chromium, tungsten, and molybdenum hexacarbonyls, Trudy Inst. Fiz. i Mat. Akad. Nauk Azerbaidzhan S.S.R. Ser. Fiz. 6 (1953) 53–61.
[55] F.A. Cotton, A.K. Fischer, G. Wilkinson, Heats of combustion and formation of metal carbonyls. I. Chromium, molybdenum and tungsten hexacarbonyls, J. Am. Chem. Soc. 78 (1956) 5168–5171, http://dx.doi.org/10.1021/ja01601a010.
[56] M.S. Sheiman, V.I. Chernova, V.V. Zakharov, I.B. Rabinovich, Thermal chemistry of chromium hexacarbonyl, Tr. Khim. Khim. Tekhnol. Gorky 1 (1974) 78–79.
[57] B. Ruscic, Active Thermochemical Tables (ATcT) Values Based on Ver. 1.122 of the Thermochemical Network, Available at, 2018, accesed: May 23 ATcT.anl.gov.